

Highly Ordered Ga Nanodroplets on a GaAs Surface Formed by a Focused Ion Beam

Qiangmin Wei,¹ Jie Lian,^{2,3} Wei Lu,⁴ and Lumin Wang^{1,5,*}

¹Department of Materials Science and Engineering, University of Michigan, Ann Arbor, Michigan 48109, USA

²Department of Geological Sciences, University of Michigan, Ann Arbor, Michigan 48109, USA

³Department of Mechanical, Aerospace and Nuclear Engineering, Rensselaer Polytechnic Institute, Troy, New York 12180, USA

⁴Department of Mechanical Engineering, University of Michigan, Ann Arbor, Michigan 48109, USA

⁵Department of Nuclear Engineering and Radiological Science, University of Michigan, Ann Arbor, Michigan 48109, USA

(Received 16 October 2007; published 21 February 2008)

The morphological evolution of a GaAs surface induced by a focused ion beam (FIB) has been investigated by *in situ* electron microscopy. Under off-normal bombardment without sample rotation, Ga droplets with sizes from 70 to 25 nm in diameter on the GaAs surface can self-assemble into a highly ordered hexagonal pattern instead of Ostwald ripening or coalescence. The mechanism relies on a balance between anisotropic loss of atoms on the surface of droplets due to sputtering and an anisotropic supply of atoms on the substrate surface due to preferential sputtering of As. The ratio of wavelength to the droplet diameter predicted by this model is in excellent agreement with experimental observations.

DOI: [10.1103/PhysRevLett.100.076103](https://doi.org/10.1103/PhysRevLett.100.076103)

PACS numbers: 68.35.B-, 61.80.Az, 79.20.Rf, 81.16.Rf

With wide applications in sensors, optical devices, and magnetic storage media, self-assembled nanostructures have attracted great interest in recent years [1–6]. Self-assembly is typically induced at temperatures below the melting point of particles, resulting in mechanically weak and often thermally and chemically unstable arrays [7,8]. It is well-known that close to the melting point, Ostwald ripening or coalescence often leads to nonuniform particle sizes during particle growth. Here, we report that this normal physical behavior can be hindered under low-energy ion bombardment, and highly ordered and uniform hexagonal patterns can be induced. The formation of ordered quantum dots by low-energy ion sputtering on a surface has been reported in several semiconductor systems. Under normal incidence or off-normal incidence with simultaneous rotation of the samples, Si [9], Ge [10], as well as a variety of III–V compounds (GaSb [11], InP [12], and InSb [13]) can form quantum dots on the surface. The mechanism involves the balance between roughening and smoothing actions, such as curvature dependent sputtering [14–16], thermal diffusion [17], redeposition and ion induced diffusion [18–20], and viscous flow [21,22]. In these processes, the conelike dots come from ion etching of the substrate, thus having the same composition as the matrix and containing high density of defects [11], and the degree of ordering is low. In this Letter, we show that, close to the melting point, the dynamic balance of mass loss and gain induced by low energetic ion bombardment can drive particles into highly ordered patterns.

Commercially available wafers of GaAs single crystal with (100) orientation were used in our work. The ion bombardment experiments were carried out using a scanning electron microscope (SEM) equipped with a focused ion beam (FIB) instrument (FEI Nova 200 Nanolab, Ga⁺ ion) in a vacuum of 2×10^{-7} mbar at room temperature (close to the Ga melting point). The surface morphology

was characterized by *in situ* SEM and *ex situ* transmission electron microscopy (TEM).

Figure 1 shows the evolution of droplets on the GaAs surface subjected to 5 keV Ga⁺ at fluence of 4.5×10^{17} cm⁻² (5 minutes) and various incident angles. At normal bombardment [Figs. 1(a) and 1(b)], droplets with diameter up to 350 nm are observed, with the droplet size following a Gaussian distribution. The mechanism of droplet formation can be attributed to the preferential sputtering of As and clustering of the remaining Ga on the surface from both substrate and ion implantation. The composition of droplets can be identified as pure Ga by energy dispersive x-ray spectrometry (EDS) analysis of the cross section sample using TEM [Fig. 2(e)]. *In situ* movie images [23] show these clusters at normal bombardment undergo random walk and encounter collisions accompanied by liquid-like coalescence. The movement of droplets is a result of the dynamic bias from the sputtering of droplets, absorption of atoms along periphery, or combination of droplets.

At off-normal bombardment [Figs. 1(c)–1(h)], however, the droplets become uniform and nearly immobile, exhibiting a tendency to form regular sixfold patterns with increasing incident angle. Starting from the appearance of small domain of ordered droplets at low incident angle, the chain of droplets with fairly constant separation is obtained at incident angle larger than 30°. The chains of droplets which are always perpendicular to the projected ion beam direction shows that ordering is independent of the orientation of the substrate. We observe through *in situ* movies [23] that Brownian motion at normal bombardment is replaced by slightly directional walk at off-normal bombardment: a movement towards the projected ion beam direction in a zigzag manner.

The temporal evolution of the highly ordered dot is investigated at fixed incident angle, energy and flux (Fig. 2). At an ion fluence of 3×10^{16} cm⁻², equivalent to an exposure time 20 s, small dots with an average

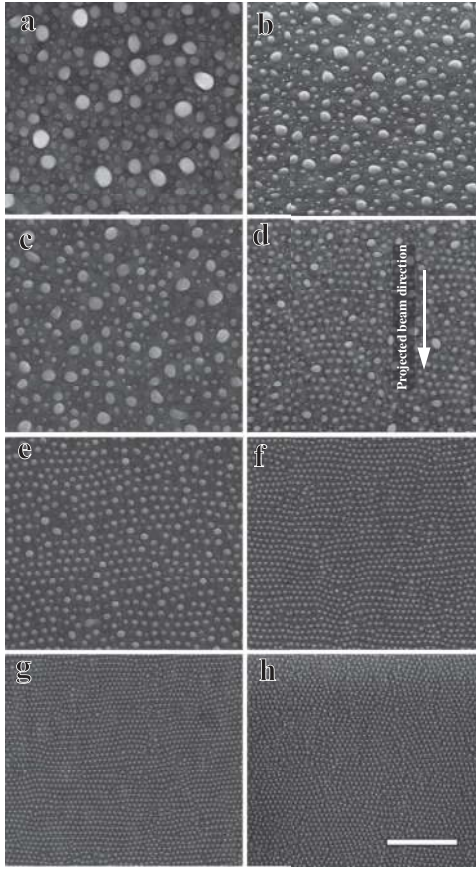


FIG. 1. SEM images of morphological evolution of GaAs at various incident angles: (a) 0° , (b) 0° , viewed from 52° to sample normal, (c) 20° , (d) 25° , (e) 30° , (f) 40° , (g) 50° , (h) 60° . Ion energy 5 keV, flux $1.5 \times 10^{15} \text{ cm}^{-2} \text{ s}^{-1}$, bombardment time 5 minutes, scale bar $1 \mu\text{m}$.

diameter of 50 nm appear, without preferred orientation and ordering. Further bombardment for 40 s, up to fluence of $9 \times 10^{16} \text{ cm}^{-2}$, leads to visible short range ordering [Fig. 2(a)]. Continuous bombardment extends the ordered domain to the whole area. The edge dislocation is evident in the image [Figs. 2(b) and 2(c)].

The mechanism underlying the pattern formation can be understood on the basis of sputtering and mass transportation. First, we should explain why the uniform droplets can be produced at off-normal bombardment. We know that the size of droplets is determined by the competition between the loss of atoms from the droplet induced by sputtering and gain of atoms supplied by the substrate. At off-normal bombardment, we can assume each droplet is surrounded by a local capture area or denuded zone in which all the Ga atoms generated in this zone is collected by surrounded droplet. For simplicity, the denuded zone is assumed to be a circle with radius of λ . If we further assume that accommodation coefficients are unity, at steady state, we have two balances: in the denuded zone, the loss of atoms to the droplets is compensated by the production within this area; for the droplet, all the atoms generated in the denuded zone are equal to the number of sputtered atoms from the

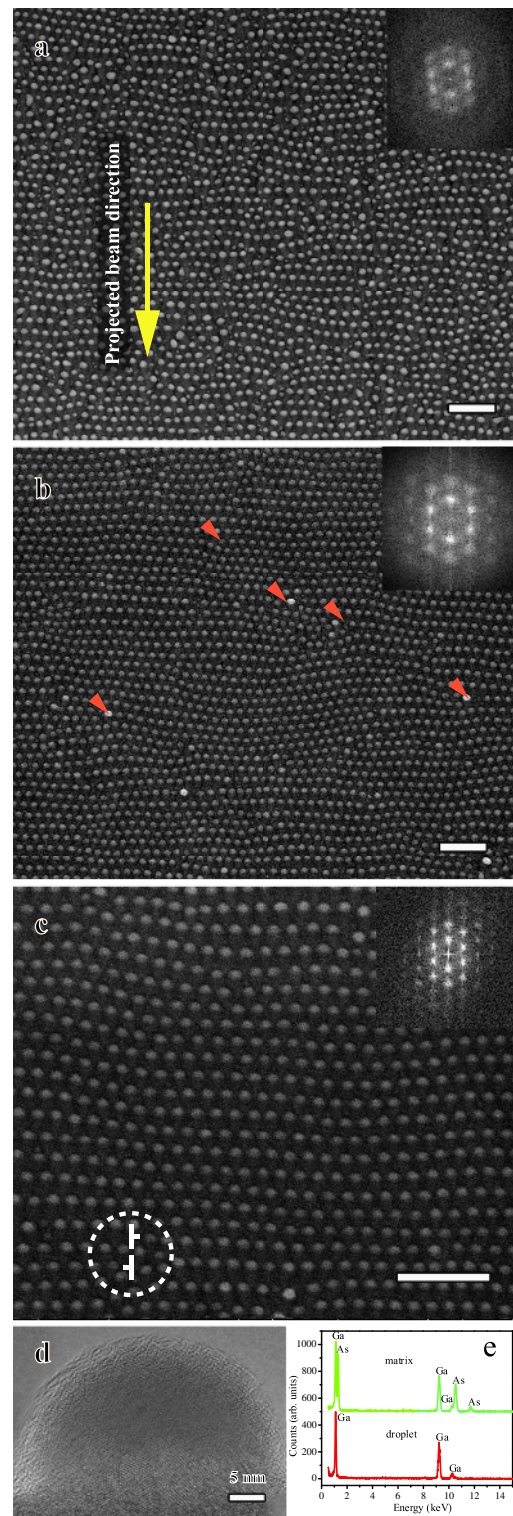


FIG. 2 (color online). Droplet development at various bombardment time (SEM images): (a) 1 minute, (b) 20 minutes, (c) 30 minutes. High density of edge dislocations can be identified in (b), as indicated by small arrows. Insets are the Fast Fourier Transformation (FFT) spectrum. Dashed circle in (c) shows two opposite edge dislocations. (d) Cross-sectional TEM image of one droplet. (e) EDS showing the composition of droplets. Ion energy 5 keV, flux $1.5 \times 10^{15} \text{ cm}^{-2} \text{ s}^{-1}$, incident angle 35° , scale bar 500 nm.

droplet. The first condition gives an equation describing the evolution of radius with respect to time. The quasistationary approximation is

$$\frac{dR}{dt} = A \left(1 - \frac{R^*}{R} + BR^2 \right) \quad (1)$$

where R is the droplet radius, A is a positive parameter, R^* is critical radius without sputtering, and B is a sputtering dependent parameter. This equation is determined by the solution of the diffusion equation in polar coordinations with a source term representing production of the Ga atoms within the capture volume. If $B = 0$, Eq. (1) reduces to a standard kinetic equation describing the process of Ostwald ripening driven by capillary induced diffusion with the mass conservation [24]. If we consider the sputtering on the droplet, we find $B < 0$. The growth rate starts to change from positive to negative when the radius reaches a certain value. This means that the radius can reach a steady state, leading to the uniform droplets. This mechanism is the key issue for the ordered pattern formation.

Another balance, where all the production of Ga atoms in the capture surface are absorbed by the droplet and these absorbed Ga atoms are equal to the sputtered Ga atoms on the surface of droplet, can demonstrate the relationship between droplet and its denuded zone. For off-normal bombardment with incident angle θ , by considering shadow effects, we have equation

$$\frac{\lambda}{R} = \sqrt{4\alpha + \cos^{-1}\theta} \quad (2)$$

where $\alpha = (Y_{\text{Ga}} - 1/2)/(Y_{\text{Ga}} + 2\zeta)$, Y_{Ga} is the sputtering yield of pure Ga bombarded by Ga ions, ζ is the fraction of implanted Ga ions staying on the substrate surface. Taking $Y_{\text{Ga}} \approx 5$ [25], $\zeta = 0.1$ [26], we get $\lambda/R = 2.15\text{--}2.4$ for incident angle $30^\circ\text{--}65^\circ$. This result is in excellent agreement with the experimental observations as shown in Fig. 3.

Inside exclusion area, the length λ is characterized by the half mean diffusion distance $\sqrt{D\tau}$, where D is ion-enhanced diffusion coefficient, τ is the average life time of atoms. The normalized flux $(f/D)^{-\psi}$ is used to describe the scaling property of mean diffusion length, where f is flux of deposition. The value of ψ is $1\text{--}1/6$, depending on the ratio of f/D [27]. If we consider the production of Ga atoms on the surface induced by the ion beam as deposition process, the decrease of droplet radius with the incident angle can be ascribed to the flux increasing with incidence.

Motivated by the convection induced self-assembly of colloidal particles [28] and one dimensional interstitial diffusion induced void lattice inside metals by high energy ion bombardment [29,30], we propose a model for self-assembly based on directional mass loss and gain. It is known that for low-energy etching, the average energy distribution approximately satisfies the Gaussian distribution [15]. At normal bombardment, the energy deposited on the surface is isotropy for sputtering. Thus, there is no

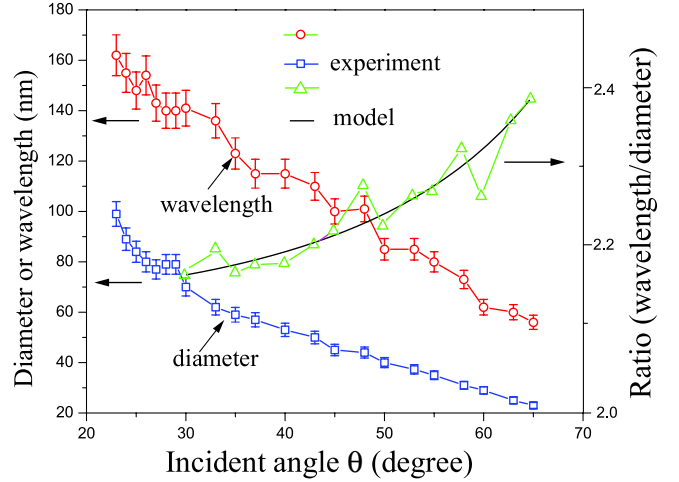


FIG. 3 (color online). Evolution of droplet diameter and wavelength with incident angles and comparison of model [Eq. (2)] with experimental data for the ratio of diameter to wavelength.

preferential migration direction for Ga atoms on the surface of GaAs induced by the ion beam, giving rise to the random walking of droplets. At off-normal bombardment, however, the deposited energy on the surface is anisotropic: it has a symmetry axis perpendicular to the projected ion beam direction, but along the projected beam direction, there exists a net force acting on the Ga atoms in a manner analogous to the wind on the surface of water [Fig. 4(a)]. This driving force tends to push the Ga atoms moving along the projected ion beam direction. On the other hand, the loss of atoms by sputtering on the surface of droplet is also directional: on the part of droplets which face the ion beam direction. In addition, because of shadowing and exclusion zone effects, only migrating atoms generated between the droplets can have much higher flux to reach the droplets in an adjacent chain. Therefore, the supply of atoms can drive the droplets to adjust their position to the site which can obtain the largest source as shown in Fig. 4(b). The center of mass driven by the competition of supply and loss of Ga atoms can move towards the projected ion beam direction in a zigzag manner as we observed in *in situ* electron microscopy. For a long time bombardment, when the droplets finish adjusting their position, the hexagonal pattern can be formed by the interaction of sputtering and anisotropy mass transport. High density of droplets, uniform size and mobility which are prerequisites for the formation of patterns, are successfully fulfilled by the ion beam [31].

The ripple formation and ripple-nanodot transition can be explained by Bradley-Harper model or extended models [14,16,18]. These models are based on instability of surface and only apply to the patterns which are of the substrate material. In our case, the dots which are liquid and separated from the substrate have a different composition with substrate. Under off-normal bombardment without rotation of sample, no Ga ripple was observed, which is contrary to the predictions of Bradley-Harper model. Our

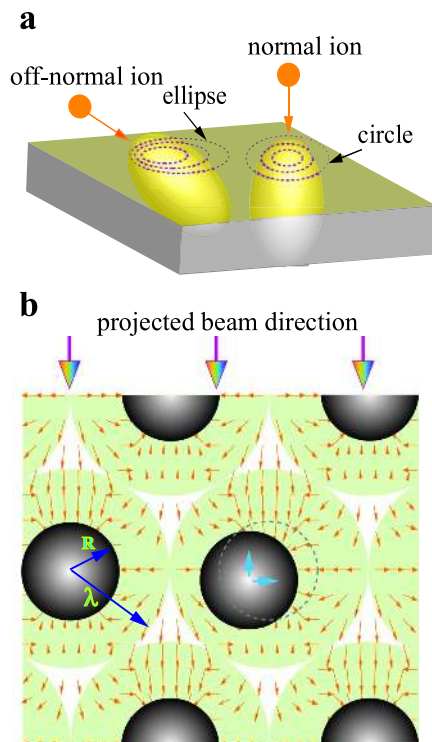


FIG. 4 (color online). Schematic illustration of a model for the formation of ordered droplet patterns. (a) Average energy distribution for ion bombardment. For normal bombardment, the deposited energy on the surface is circular, while for off-normal bombardment, it is elliptical where the energy contour along the projected beam direction is longer than other directions. The dashed curves represent the equal energy contours. (b) Atom supply and movement directions that cause an off-center particle to move to the center of nanoparticle lattice. Small arrows represent the direction and magnitude of local Ga atom migration induced by the ion beam on the substrate surface, radial dark shaded circle denotes the droplet, the light circle with radius λ is the exclusive zone for Ga, arrows inside droplet indicate the movement direction of droplets, and dashed circle shows the final position of partially aligned droplets.

model is based on high density of dots on the surface. It can apply to patterns whose density is high enough that small adjustment can lead to the hexagonal pattern formation, similar to void lattice formation and highly ordered colloidal particle formation.

In conclusion, we have characterized the formation of a highly ordered, hexagonal pattern of Ga nanodroplets on the surface of single crystal GaAs induced by off-normal FIB without sample rotation. We proposed, at the melting point, the dynamic balance of directional mass loss and gain can drive droplets into highly ordered patterns. The sputtering induced droplet patterns presented here have potential applications in investigating fundamental physical phenomena, such as sputtering effect on the deposition, diffusion and aggregation model.

This work was supported by the Office of Basic Energy Sciences of the U.S. Department of Energy under Grant

No. DE-FG02-02ER46005.

*Corresponding author: lmwang@umich.edu

- [1] M. L. Anderson, N. C. Bartelt, P. J. Feibelman, B. S. Swartzentruber, and G. L. Kellogg, *Phys. Rev. Lett.* **98**, 096106 (2007).
- [2] E. V. Shevchenko *et al.*, *Nature (London)* **439**, 55 (2006).
- [3] P. F. A. Alkemade, *Phys. Rev. Lett.* **96**, 107602 (2006).
- [4] J. Muñoz-García, M. Castro, and R. Cuerno, *Phys. Rev. Lett.* **96**, 086101 (2006).
- [5] A.-D. Brown, J. Erlebacher, W. L. Chan, and E. Chason, *Phys. Rev. Lett.* **95**, 056101 (2005).
- [6] H. H. Chen *et al.*, *Science* **310**, 294 (2005).
- [7] H. Fan *et al.*, *Science* **304**, 567 (2004).
- [8] F. X. Redl, K. S. Cho, C. B. Murray, and S. O'Brien, *Nature (London)* **423**, 968 (2003).
- [9] R. Gago *et al.*, *Phys. Rev. B* **73**, 155414 (2006).
- [10] B. Ziberi, F. Frost, and B. Rauschenbach, *Appl. Phys. Lett.* **88**, 173115 (2006).
- [11] S. Facsko *et al.*, *Science* **285**, 1551 (1999).
- [12] F. Frost, A. Schindler, and F. Bigl, *Phys. Rev. Lett.* **85**, 4116 (2000).
- [13] F. Frost, B. Ziberi, T. Höche, and B. Rauschenbach, *Nucl. Instrum. Methods Phys. Res., Sect. B* **216**, 9 (2004).
- [14] R. Bradley and J. Harper, *J. Vac. Sci. Technol. A* **6**, 2390 (1988).
- [15] P. Sigmund, *Phys. Rev.* **184**, 383 (1969).
- [16] R. Cuerno and A.-L. Barabási, *Phys. Rev. Lett.* **74**, 4746 (1995).
- [17] W. W. Mullins, *J. Appl. Phys.* **28**, 333 (1957).
- [18] M. Castro, R. Cuerno, L. Vázquez, and R. Gago, *Phys. Rev. Lett.* **94**, 016102 (2005).
- [19] J. Erlebacher, M. J. Aziz, E. Chason, M. B. Sinclair, and J. A. Floro, *Phys. Rev. Lett.* **82**, 2330 (1999).
- [20] M. Makeev, R. Cuerno, and A.-L. Barabási, *Nucl. Instrum. Methods Phys. Res., Sect. B* **197**, 185 (2002).
- [21] E. Chason, T. M. Mayer, B. K. Kellerman, D. T. McIlroy, and A. J. Howard, *Phys. Rev. Lett.* **72**, 3040 (1994).
- [22] S. G. Mayr and R. S. Averbach, *Phys. Rev. Lett.* **87**, 196106 (2001).
- [23] See EPAPS Document No. E-PRLTAO-100-026808 for movies and a supplementary appendix. For more information on EPAPS, see <http://www.aip.org/pubservs/epaps.html>.
- [24] B. K. Chakraverty, *J. Phys. Chem. Solids* **28**, 2413 (1967).
- [25] J. F. Ziegler, J. P. Biersack, and U. Littmark, *The Stopping and Range of Ions in Solids* (Pergamon Press, New York, 1985).
- [26] H. H. Anderson, in *Ion Implantation and Beam Processing*, edited by J. S. Williams and J. M. Poate (Academic Press, New York, 1984).
- [27] P. Jensen, A. L. Barabasi, H. Larralde, S. Havlin, and H. E. Stanley, *Phys. Rev. E* **50**, 618 (1994).
- [28] Z. Mitov and E. Kumacheva, *Phys. Rev. Lett.* **81**, 3427 (1998).
- [29] A. J. E. Foreman, Atomic Energy Research Establishment Report No. AERE-R-7135, 1972.
- [30] C. H. Woo and W. Frank, *J. Nucl. Mater.* **137**, 7 (1985).
- [31] G. M. Whitesides and B. Grybowski, *Science* **295**, 2418 (2002).